OPEN

NPG Asia Materials (2017) 9, e359; doi:10.1038/am.2017.20
www.nature.com/am

ORIGINAL ARTICLE

Conversion of an ultra-wide bandgap amorphous oxide insulator to a semiconductor

Junghwan Kim[1,2], Takumi Sekiya[1], Norihiko Miyokawa[1], Naoto Watanabe[1], Koji Kimoto[3], Keisuke Ide[1], Yoshitake Toda[2], Shigenori Ueda[3,4], Naoki Ohashi[2,5], Hidenori Hiramatsu[1,2], Hideo Hosono[1,2] and Toshio Kamiya[1,2]

The variety of semiconductor materials has been extended in various directions, for example, to very wide bandgap materials such as oxide semiconductors as well as to amorphous semiconductors. Crystalline β-Ga_2O_3 is known as a transparent conducting oxide with an ultra-wide bandgap of ~4.9 eV, but amorphous (a-) Ga_2O_x is just an electrical insulator because the combination of an ultra-wide bandgap and an amorphous structure has serious difficulties in attaining electronic conduction. This paper reports semiconducting a-Ga_2O_x thin films deposited on glass at room temperature and their applications to thin-film transistors and Schottky diodes, accomplished by suppressing the formation of charge compensation defects. The film density is the most important parameter, and the film density is increased by enhancing the film growth rate by an order of magnitude. Additionally, as opposed to the cases of conventional oxide semiconductors, an appropriately high oxygen partial pressure must be chosen for a-Ga_2O_x to reduce electron traps. These considerations produce semiconducting a-Ga_2O_x thin films with an electron Hall mobility of ~8 $cm^2V^{-1}s^{-1}$, a carrier density N_e of ~2×10^{14} cm^{-3} and an ultra-wide bandgap of ~4.12 eV. An a-Ga_2O_x thin-film transistor exhibited reasonable performance such as a saturation mobility of ~1.5 $cm^2V^{-1}s^{-1}$ and an on/off ratio $>10^7$.

NPG Asia Materials (2017) **9,** e359; doi:10.1038/am.2017.20; published online 10 March 2017

INTRODUCTION

Carrier doping and consequent control of carrier density are essential requirements for semiconductors. Therefore, carrier doping to a known insulating material has been a guiding principle in developing new semiconductors. However, it is difficult to dope carriers to a wide bandgap material, as explained, for example, by the intrinsic doping limit.[1] Developing new amorphous semiconductors is another area of interest because amorphous semiconductors can be fabricated even at room temperature on plastic and are applicable to flexible devices. However, obtaining electron conduction in an amorphous material is much more difficult than obtaining electron conduction in a crystalline material. Only hydrogenated amorphous silicon and amorphous oxide semiconductors (AOSs) have been utilized as active layers in practical semiconductor devices.[2]

Developing an ultra-wide bandgap amorphous semiconductor is very challenging and also interesting from the viewpoint of materials science. It is important also for practical applications because such materials will allow us to integrate power devices with large-size glass and flexible substrates. β-Ga_2O_3 is a crystalline semiconductor with an ultra-wide bandgap of ~4.9 eV[3] and has recently been examined for applications in deep-ultraviolet devices[4] and power devices.[5] Although carrier doping in β-Ga_2O_3 has been difficult, as recently explained by theoretical calculations,[6] impurity doping using Sn or Si has been discovered to attain electronic conduction,[1,7] which has widened the range of applications of β-Ga_2O_3, for example, to power devices. However, although a large number of AOS materials with bandgaps of ~3.0 eV, such as a-In-Ga-Zn-Sn-O, have been developed to date,[2,8,9] semiconducting behavior has never been observed for amorphous Ga_2O_x (a-Ga_2O_x); only ionic conduction and an insulator-metal transition at a high temperature have been reported.[10,11] A reason for this difficulty is that aliovalent ion doping does not work for amorphous semiconductors except for hydrogenated amorphous silicon; therefore, only metal/oxide ion off-stoichiometry and hydrogen doping would be effective doping methods in AOSs, and consequently carrier control of the conventional AOSs has been conducted mainly by controlling oxygen partial pressure during deposition and thermal annealing (P_{O2}) as well as by hydrogen doping.[12] Even these conventional doping methods could not produce semiconducting a-Ga_2O_x.

Here we have succeeded in fabricating semiconducting a-Ga_2O_x thin films on glass at room temperature. A key strategy is opposite

[1]Laboratory for Materials and Structures, Institute of Innovative Research, Tokyo Institute of Technology, Yokohama, Japan; [2]Materials Research Center for Element Strategy, Tokyo Institute of Technology, Yokohama, Japan; [3]Quantum Beam Unit, National Institute for Materials Science, Ibaraki, Japan; [4]Synchrotron X-ray Station at SPring-8, National Institute for Materials Science, Hyogo, Japan and [5]National Institute for Materials Science, Ibaraki, Japan
Correspondence: Professor J Kim, Materials Research Center for Element Strategy, Tokyo Institute of Technology, Mailbox SE-6, 4259 Nagatsuta, Midori-ku, Yokohama 226-8503, Japan.
E-mail: JH.KIM@lucid.msl.titech.ac.jp
or Professor T Kamiya, Laboratory for Materials and Structures, Institute of Innovative Research, Tokyo Institute of Technology, Mailbox R3-4, 4259 Nagatsuta, Midori-ku, Yokohama 226-8503, Japan.
E-mail: kamiya.t.aa@m.titech.ac.jp
Received 14 November 2016; revised 5 January 2017; accepted 7 January 2017

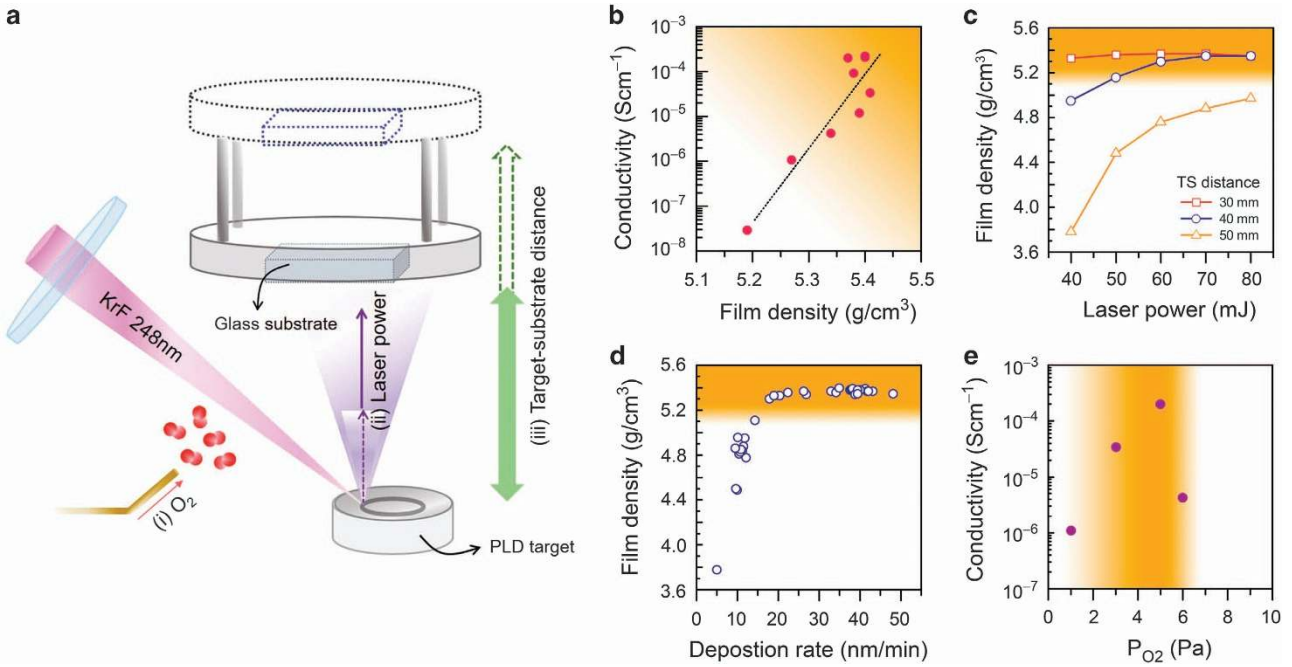

Figure 1 Relation between electronic conduction and film density. (**a**) Deposition parameters affecting the film structures and properties such as (i) P_{O2}, (ii) laser power and (iii) TS distance. (**b**) Electrical conductivity vs film density, indicating that film densities $\geqslant 5.2\,g\,cm^{-3}$ are required to obtain semiconducting films. (**c**) Film density vs laser power and TS distance. (**d**) Replot of panel (**b**) with respect to deposition rate, giving a single universal curve between deposition rate and film density. (**e**) P_{O2} dependence of conductivity, showing that too low (<1 Pa) and too high P_{O2} (>6 Pa) produced insulating films only.

to the strategy for conventional oxide semiconductors where a lower P_{O2} is chosen to obtain a higher electron density and better conductivity. Another important key is to increase the film growth rate to obtain a higher film density so that formation of electron traps is suppressed. Furthermore, incorporation of weakly bonded or excess oxygen should also be suppressed. Thus semiconducting a-Ga_2O_x thin films were obtained with an electron Hall mobility of $\sim 8\,cm^2\,V^{-1}\,s^{-1}$, a carrier density of $\sim 2\times10^{14}\,cm^{-3}$ and a bandgap of ~ 4.12 eV, which produced operating semiconductor devices including thin-film transistors (TFTs) and Schottky diodes.

MATERIALS AND METHODS

a-Ga_2O_x films were fabricated by pulsed laser deposition (PLD) using a KrF excimer laser (wavelength: 248 nm) in an O_2 gas flow on silica glass substrates at room temperature. The back pressure for PLD was $\sim 2\times10^{-6}$ Pa. We synthesized polycrystalline targets of β-Ga_2O_3, $(Ga_{0.35}Zn_{0.65})_2O_x$ and $(Ga_{0.7}Zn_{0.3})_2O_x$ from powdered reagents of ZnO (purity 99.999%) and Ga_2O_3 (purity 99.99%) by sintering at 1400 °C for 5 h in air. P_{O2} during deposition and laser power were varied from 0 to 10 Pa and from 30 to 80 mJ, respectively. Some films were subjected to postdeposition thermal annealing at $T_a = 200$–600 °C in vacuum, dry O_2 and H_2 gas flows.

Film structures and thicknesses were characterized and determined by high-resolution transmission electron microscopy, X-ray diffraction and grazing-incidence X-ray reflectivity spectroscopy, which confirmed that all of the films examined in this study were amorphous (see X-ray diffraction, high-resolution transmission electron microscopy and grazing-incidence X-ray reflectivity in Supplementary Figures S1–S3, respectively). Optical bandgap values (E_g) were estimated by Tauc' plots for the amorphous films.

Electrical properties were measured by the Hall effect with the van der Pauw configuration. Desorption of the film constituents and impurity-related species was measured by thermal desorption spectroscopy (TDS). For the TDS measurement, ~140-nm-thick a-Ga_2O_x films were deposited under different deposition conditions. Then the samples were taken out to the air once from the PLD deposition chamber and then introduced into the TDS measurement chamber. The back pressure of the TDS chamber was $\sim 2\times10^{-7}$ Pa.

Chemical composition (Ga:O ratio) was determined using an electron-probe microanalyzer equipped with a field-emission-type electron gun and a wavelength dispersive X-ray detector. Hard X-ray photoemission spectroscopy (HAXPES) measurements at room temperature were performed using the BL15XU undulator beamline (the excitation X-ray energy: $h\nu = 5953.4$ eV)[13,14] of SPring-8. The binding energy was calibrated with the E_F of an evaporated Au thin film, and the total energy resolution was set to 240 meV, which was confirmed by the Fermi cutoff of the Au film. The energy levels of the conduction band minimum (CBM, E_{CBM}) and the valence band maximum (VBM, E_{VBM}) from the vacuum level (E_{VAC}) ($E_{VAC} - E_{CBM}$ and $E_{VAC} - E_{VBM}$ are electron affinity, χ, and ionization potential, I_p, respectively) were measured by ultraviolet photoemission spectroscopy (UPS) (excited by He I and II light sources). To prepare chemically pure surfaces for the UPS measurements, Ar ion sputtering was conducted for 1 h at an acceleration voltage of 1 kV. Work function was determined from the cutoff energy of secondary electrons, and I_p was estimated by combining E_{VAC} and the measured E_{VBM} (see Supplementary Figure S4). χ was speculated using the measured optical bandgap by $\chi = I_p + E_g$.

Bottom-gate, top-contact TFTs were fabricated using semiconducting a-Ga_2O_x channels on SiO_2/n^+-Si substrates (see Figure 5a for the device structure). The a-Ga_2O_x layers were deposited at room temperature, followed by thermal annealing at 200 °C under vacuum. Finally, aluminum source/drain contacts were deposited by thermal evaporation. A-Ga_2O_x/Pt Schottky diodes were fabricated on Pt/silica glass substrates, finished by evaporating aluminum top Ohmic contacts (Figure 5c).

RESULTS AND DISCUSSION

Controlling factor to obtain semiconducting a-Ga_2O_x

In the beginning of this work, we employed film growth conditions that were similar to device-quality a-In-Ga-Zn-O (a-IGZO) for

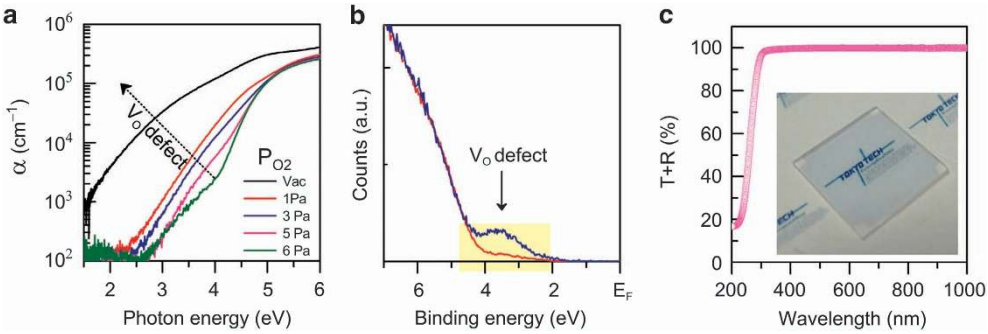

Figure 2 Subgap defects in a-Ga_2O_x. (**a**) Optical absorption spectra as a function of P_{O2} from 0 to 6 Pa. (**b**) HAXPES spectra around the bandgap region for conducting and insulating films deposited at $P_{O2}=6$ Pa (the red curve) and 1 Pa (the black curve), respectively. The binding energy is measured from the Fermi level, and the VBMs are located at ~4.1 eV. (**c**) Transmittance+reflectance spectra and photo of the conducting a-Ga_2O_x film of ~120 nm thickness.

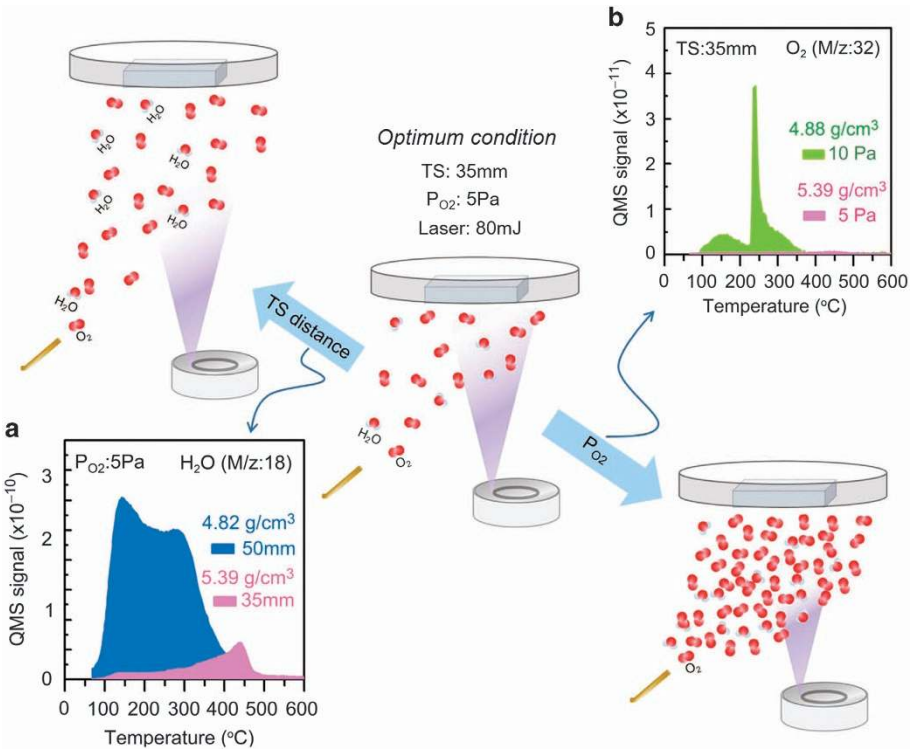

Figure 3 Schematic illustration of the effects of deposition parameters (TS distance and P_{O2}) on incorporation of impurity species. (**a**, **b**) TDS spectra of (**a**) H_2O (TS distances are 50 mm for blue and 35 mm for purple) and (**b**) O_2 (P_{O2} are 10 Pa for green and 5 Pa for purple). The TS distance of 35 mm and the $P_{O2}=5$ Pa are the optimum conditions and produced the high-density semiconducting a-Ga_2O_x film.

PLD (that is, P_{O2} of 1–5 Pa, target-substrate (TS) distance of 50 mm and laser power of 50 mJ) because these a-IGZO films produce good TFTs and have low defect densities even when deposited at room temperature on glass.[15,16] However, all of the a-Ga_2O_x films thus fabricated were insulators with electrical conductivities below the measurement limit of our apparatus ($<10^{-8}$ S cm^{-1}), although we had examined wider deposition conditions from $P_{O2}=0$ Pa and performed several postdeposition treatments such as thermal annealing in vacuum, O_2, and H_2 because these are standard procedures to dope electrons onto oxide semiconductors.

By investigating further wider deposition conditions including the TS distance and the laser power, we finally found the deposition conditions to obtain electron conduction as shown in Figure 1. Electrical conductivities were obtained only if the film density was >5.2 g cm^{-3} (Figures 1b and c), where the electrical conductivity increased exponentially with the increase in the film density. Figure 1c, in which the films exhibiting electrical conductivity are shown by the orange shaded region, shows that the TS distance and laser power are not the essential controlling factors because the smallest TS distance of 30 mm produced conducting films independent of the laser power, but the larger TS distances failed to attain conductivity, particularly for low laser power. Replotting these data with respect to the deposition rate (Figure 1d) gives a single universal curve, indicating that the film density is the essential controlling factor. The deposition rates for device-quality a-IGZO

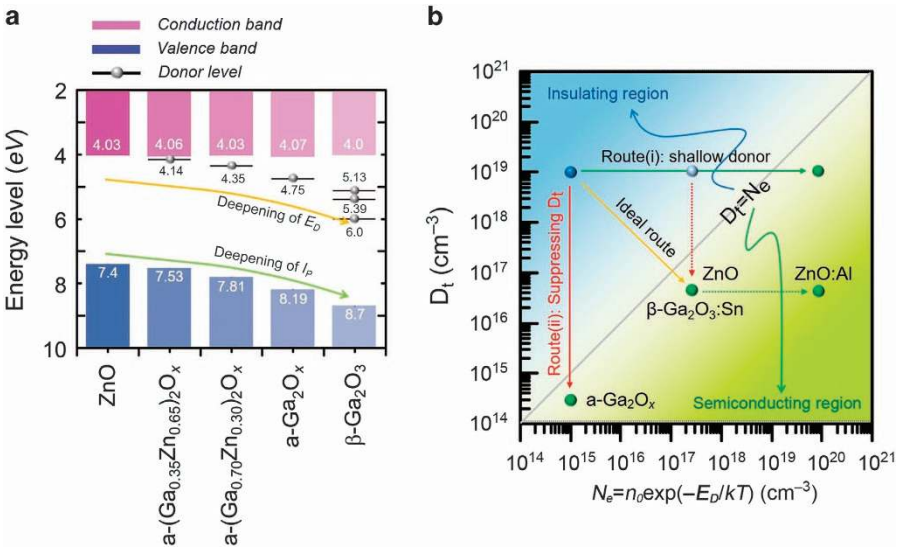

Figure 4 (**a**) Band alignment diagram of a-$(Ga_{1-y}Zn_y)_2O_x$ in comparison with crystalline ZnO built from E_g and UPS results in Supplementary Figure S4 of the supporting information. The values for ZnO and β-Ga_2O_3 are taken from Klein[23] and Mohamed and Schottky[24], respectively. The E_D value for β-Ga_2O_3 is taken from Varley *et al.*[6] E_{VBM} (ionization potential, I_P) is shown by the top edges of the blue bars and E_{CBM} (electron affinity, χ) by the bottom edges of the purple bars. E_D levels are also shown by the horizontal bars with spheres. (**b**) The schematic diagram shows routes to convert an insulator to a semiconductor.

films are ~5 nm min^{-1}, and the deposition rates required for semiconducting a-Ga_2O_x films are larger by one to several orders of magnitude.

P_{O2} is also an essential controlling parameter to attain conducting films. We should, however, emphasize that the optimum P_{O2} obtained for a-Ga_2O_x is very different from the value for conventional oxide semiconductors for which a lower P_{O2} is required to obtain a higher electronic conduction and a higher free electron density. That is, low P_{O2} including zero (that is, in vacuum) produced insulating a-Ga_2O_x films only, and the best conductivity of ~2×10^{-4} S cm^{-1} was obtained at a rather high $P_{O2}=5$ Pa. This value can be explained from the subgap defects observed in optical absorption spectra (Figure 2a) and HAXPES spectra around the bandgap region (Figure 2b). Similar to previous reports,[10,17] the low P_{O2} films seem to have small apparent E_g due to subgap absorption, but the actual E_g is estimated to be 4.12 eV from the Tauc' plot of the $P_{O2}=6$ Pa film because it has the smallest subgap absorption. Strong subgap absorption extends from $E_g=4.12$ to 0.5 eV for the $P_{O2}=0$ film. The subgap absorption originates from the subgap defects just above the VBM (near-VBM states) as seen in the HAXPES spectra in Figure 2b, where the VBM level is estimated to be ~4.1 eV from the Fermi level (E_F) by extrapolating the straight VB tail to zero. The film deposited at a low $P_{O2}=1$ Pa (the film density of 5.27 g cm^{-3}) shows high-density peak-shape near-VBM states (denoted 'V_O defect' for the black curve), while the film deposited at the optimum $P_{O2}=6$ Pa (5.39 g cm^{-3}) has much smaller near-VBM states (the red curve). These results are similar to previously reported a-IGZO cases and explain that a low P_{O2} condition produces electron traps, probably due to oxygen deficiency with free space (void) structures.[18] This result explains the P_{O2} vs conductivity result in Figure 1e because lower P_{O2} may generate free electrons due to oxygen deficiency as usual for oxide semiconductors, while it also produces the near-VBM defects and these defects trap all the generated electrons, leading to the stronger charge compensation at lower P_{O2} and consequently to the insulating films.

The next question is why the film deposition rate determines the film density as seen in Figure 1d. TDS spectra in Figures 3a and b show that the film density is altered largely by the TS distance and P_{O2}. The low-density film deposited at a large TS distance of 50 mm exhibited high-density desorption of H_2O molecules even from the very low temperature of ~80 °C, implying that lower density films incorporate more impurities such as H_2O, OH and H-related molecules. This result suggests that the low density would come from incorporation of residual H_2O and H-related molecules in the PLD chamber because a lower growth rate requires a longer deposition time and incorporates more impurity from the deposition atmosphere into the growing film as illustrated in Figure 3. There is another important factor to determine the film density; a higher deposition rate condition would produce deposition precursors with higher kinetic energies, which enhances structural relaxation in the growing surface region and assists in forming a denser structure.

Figure 1e shows that the optimum P_{O2} were 5–6 Pa, but the conductivity dropped sharply by further increasing P_{O2}, and no conducting film was obtained at >6 Pa. The O_2 TDS spectra in Figure 3b show that the film deposited at the optimum condition of $P_{O2}=5$ Pa did not show O_2 desorption up to 350 °C (note that this film is of high density), while the film deposited at a high $P_{O2}=10$ Pa (a low-density film) exhibited a large amount of O_2 desorption even from the low temperature of 80 °C. A similar result is observed in a-IGZO films fabricated under strong oxidation conditions, and similar low-temperature O_2 desorption is attributed to weakly bonded oxygen that forms an electron trap.[19–21] Similar to the a-IGZO case, the insulating behavior of the high P_{O2} a-Ga_2O_x films can be explained by the charge compensation due to the electron traps originating from the weakly bonded oxygen.

Electronic structure of a-Ga_2O_x

Next, we investigated the electronic structure of a-Ga_2O_x. To systematically investigate the variation of electronic structure, we compared the electronic structure of a-Ga_2O_x with the electronic structure of its

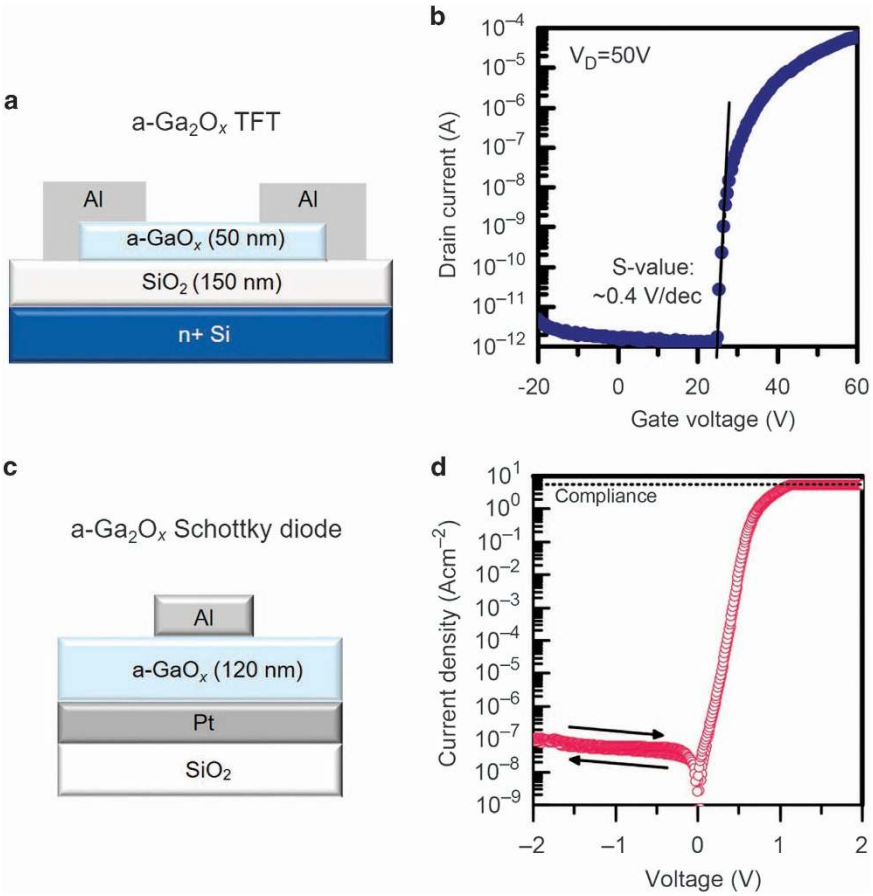

Figure 5 a-Ga_2O_x devices. (**a**) TFT structure and (**b**) transfer characteristic. (**c**) Schottly diode structure and (**d**) current–voltage characteristic.

solid-solution system a-$(Ga_{1-y}Zn_y)_2O_x$ ($y=0$, 0.30, 0.65). Their electrical properties, the temperature dependence of electrical conductivity (σ_e), electron Hall mobility (μ_e) and free electron density (n_e) are summarized in Supplementary Figure S5 and Supplementary Table S1, which substantiated that all of the films were n-type semiconductors and that their donor levels measured from the CBM deepen with the decreasing Zn content from $E_{CBM}-E_D=0.08$ to 0.32 and to 0.68 eV for a-$(Ga_{0.35}Zn_{0.65})_2O_x$ to a-$(Ga_{0.70}Zn_{0.30})_2O_x$ and to a-Ga_2O_x, respectively. The total donor densities n_0 were also estimated from the equation $n_e=n_0\ \exp(-(E_{CBM}-E_D)/(k_BT))$, providing $n_0=1.0\times10^{18}$, 1.5×10^{18} and $7.5\times10^{19}\,cm^{-3}$ for a-$(Ga_{0.35}Zn_{0.65})_2O_x$, a-$(Ga_{0.70}Zn_{0.30})_2O_x$ and a-Ga_2O_x, respectively. These densities indicate that although n_0 is the largest for a-Ga_2O_x, n_e is limited due to the deep donor level, $E_{CBM}-E_D$. All of the a-$(Ga_{1-y}Zn_y)O_x$ films exhibited rather large electron mobility for amorphous semiconductors, 6–8 $cm^2\,V^{-1}\,s^{-1}$ at room temperature, similar to a-IGZO.[15,16] This result substantiates that the low value for σ_e of a-Ga_2O_x of $\sim2\times10^{-4}\,S\,cm^{-1}$ at most originates from the low n_e, not from μ_e. This origin would be reasonable because both a-IGZO and a-GaO_x have similar CBM structures made mainly of spherical metal *s* orbitals, which can form a highly dispersed conduction band with small electron effective masses even in a disordered amorphous structure.[22]

The E_g values, which were determined from Tauc' plots (Supplementary Figure S4d), were 4.12, 3.78 and 3.47 eV for a-$(Ga_{0.35}Zn_{0.65})_2O_x$, a-$(Ga_{0.70}Zn_{0.30})_2O_x$ and a-Ga_2O_x, respectively, and the ionization potential ($I_P=E_{VBM}$) values were obtained by UPS measurements (Supplementary Figure S2). Consequently, the band alignment diagram is built as shown in Figure 4a. The diagram shows that E_{VBM} deepens as the Zn content decreases while E_{CBM} remains almost unchanged, indicating that the difference in E_g comes mostly from the deepening of E_{VBM}. This result would be unexpected because one may expect that E_{VBM} values of oxide semiconductors are similar because their VBM levels are mainly made of the common chemical states, O 2p–O 2p antibonding states, and consequently, it would be natural to expect that the Ga^{3+} 4s level, which constitutes the CBM in Ga_2O_x, lies at a shallower energy than Zn^{2+} 4s as speculated from the difference in E_g. However, this result indicates that the energy levels of the unoccupied *s* orbitals in Ga^{3+} and Zn^{2+} are similar, while E_g is determined mainly by E_{VBM}. A similar result is also reported for crystalline β-Ga_2O_3.[24] This trend is explained by an O 2p–Zn 3d interaction as reported for II–VI semiconductors;[25] that is, the Zn 3d level is shallower than Ga 3d and has a larger antibonding coupling with O 2p states, which raises E_{VBM} as the Zn content increases. The doping limit in many n-type oxides is determined by their E_{CBM} measured from the vacuum level.[26,27] Thus β-Ga_2O_3 and a-Ga_2O_x can be doped to n-type because their E_{CBM} values are close to that of ZnO and within this doping limit. We also see an interesting relation between E_D and E_{VBM} in Figure 4a. In the a-$(Ga_{1-y}Zn_y)O_x$ case, the E_D level deepens as the Zn content increases (that is, $E_{CBM}-E_D=0.08$, 0.32 and 0.68 eV for $y=0.65$, 0.30 and 0, respectively) and appears to have a stronger correlation with E_{VBM} than with E_{CBM}; that is, the E_D-E_{VBM} are almost the same at 7.45, 7.49 and 7.13 eV.

Here we discuss why the semiconductor conversion of a-Ga_2O_x was so difficult. As schematically shown in Figure 4b, good transparent conducting oxides such as Al-doped ZnO (ZnO:Al) have a high free electron concentration, for example, at $>10^{20}\,cm^{-3}$, generated from a shallow donor level of Al_{Zn}, while the electron trap density (D_t) would be negligible compared to the free electron concentration. However, the blue region in Figure 4b has high-density electron traps and/or low-density free electrons generated from the donors, producing electrical insulators. Ultra-wide bandgap amorphous materials can attain electronic conduction only with difficulty because the ultra-wide gap leads to low N_e and the amorphous structure leads to high D_t. As seen in Figure 4a, the donor level in a-Ga_2O_x is very deep at 0.68 eV and gives N_e as small as $10^{15}\,cm^{-3}$; therefore, very small $D_t > 10^{15}\,cm^{-3}$ are critical, and only insulating a-Ga_2O_x films had been obtained to date. Consequently, as shown by 'Route(ii)', the semiconducting a-Ga_2O_x films here are obtained by suppressing D_t.

Applications to semiconductor devices

The potential of the semiconducting a-Ga_2O_x films was demonstrated by fabricating TFTs (Figure 5a) and Schottky diodes (Figure 5c). The a-Ga_2O_x TFT exhibited a reasonable performance such as a saturation mobility of $\sim 1.5\,cm^2\,V^{-1}\,s^{-1}$, an on/off ratio of $>10^7$ and a subthreshold swing voltage of $\sim 0.4\,V\,dec^{-1}$ (Figure 5b). The a-Ga_2O_x/Pt Schottky diode also shows a good current–voltage characteristic with a very high on/off ratio ($>10^9$) with a negligible hysteresis (Figure 5d). Although the a-Ga_2O_x/Pt Schottky junction was reported by Aoki,[11] it operated via ion conduction in a-Ga_2O_x.

CONCLUSIONS

Semiconducting a-Ga_2O_x thin films with a bandgap of 4.12 eV were successfully fabricated on glass at room temperature, and the electronic structure was clarified in comparison with its Zn solid solutions. The keys to obtaining electronic conduction in a-Ga_2O_x are (i) a high film density and (ii) an appropriately high P_{O2} to suppress formation of electron traps. As the donor level is very deep, 0.68 eV from E_{CBM}, for a-Ga_2O_x, the free electron density is still low, $2\times10^{14}\,cm^{-3}$ at best, although the total donor density is rather high, $7.5\times10^{19}\,cm^{-3}$. The formation of a trace amount of electron traps at an order of $10^{14}\,cm^{-3}$ is therefore critical to fully compensate for the generated free carriers, making a sharp contrast with conventional oxide semiconductors. Those conventional oxides have shallow donor levels and high-density free electrons, and therefore, the effect of charge-compensating electron traps is invisible and low P_{O2} deposition conditions effectively produce high carrier density, high conductivity films. The present result shows that this strategy for conventional oxide semiconductors should be reconsidered for developing new semiconductor materials that have very wide bandgaps, deep donor/acceptor levels and/or other extreme conditions/requirements. Seeking a deposition/annealing condition/method to suppress charge compensating defects should also be considered.

This discovery, that is, the importance of controlling charge compensation, will lead to developing further new semiconductors as well as to improving carrier transport properties and device performance of known oxide semiconductors in which generating high-density carriers or obtaining high-performance devices is difficult, such as p-type oxide semiconductors.

CONFLICT OF INTEREST

The authors declare no conflict of interest.

ACKNOWLEDGEMENTS

This work was supported by the Ministry of Education, Culture, Sports, Science and Technology (MEXT) through the Element Strategy Initiative to Form Core Research Center. JK and KI were also supported by the Japan Society for the Promotion of Science (JSPS) through a Grant-in-Aid for Research Activity Start-up Grant Nos. 16H06795 and 15H06207, respectively. H Hiramatsu was also supported by Support for Tokyotech Advanced Research (STAR).

Author contributions: TK and H Hosono supervised the project. JK, TS, NM and NW fabricated and characterized the samples with support by KI and H Hiramatsu. KK performed transmission electron microscope observations. YT, SU and NO performed HAXPES measurements and their analyses. JK wrote the manuscript with contributions mainly from TK, KI and H Hiramatsu and comments from H Hosono, KK and SU. All authors have given their approval for the final version of the manuscript.

1 Walukiewicz, W. Intrinsic limitations to the doping of wide-gap semiconductors. *Physica B* **123**, 302–303 (2001).
2 Nomura, K, Ohta, H., Takagi, A., Kamiya, T., Hirano, M. & Hosono, H. Room-temperature fabrication of transparent flexible thin-film transistors using amorphous oxide semiconductors. *Nature* **432**, 488–492 (2004).
3 Orita, M., Ohta, H., Hirano, M. & Hosono, H. Deep-ultraviolet transparent conductive β-Ga_2O_3 thin films. *Appl. Phys. Lett.* **77**, 4166 (2000).
4 Matsuzaki, K., Yanagi, H., Kamiya, T., Hiramatsu, H., Nomura, K., Hirano, M. & Hosono, H. Field-induced current modulation in epitaxial film of deep-ultraviolet transparent oxide semiconductor Ga_2O_3. *Appl. Phys. Lett.* **88**, 092106 (2006).
5 Higashiwaki, M., Sasaki, K., Kuramata, A., Masui, T. & Yamakoshi, S. Gallium oxide (Ga_2O_3) metal-semiconductor field-effect transistors on single-crystal β-Ga_2O_3 (010) substrates. *Appl. Phys. Lett.* **100**, 013504 (2012).
6 Varley, J., Weber, J., Janotti, A. & Van de Walle, C. Oxygen vacancies and donor impurities in β -Ga_2O_3. *Appl. Phys. Lett.* **97**, 142106 (2010).
7 Villora, E., Shimamura, K., Yoshikawa, Y., Ujiie, T. & Aoki, K. Electrical conductivity and carrier concentration control in β-Ga_2O_3 by Si doping. *Appl. Phys. Lett.* **92**, 202120 (2008).
8 Chiang, H., Wager, J., Hoffman, R., Jeong, J. & Keszler, D. High mobility transparent thin-film transistors with amorphous zinc tin oxide channel layer. *Appl. Phys. Lett.* **86**, 013503 (2005).
9 Ogo, Y., Nomura, K., Yanagi, H., Kamiya, T., Hirano, M. & Hosono, H. Amorphous Sn–Ga–Zn–O channel thin-film transistors. *Phys. Stat. Sol. (A)* **205**, 1920–1924 (2008).
10 Nagarajan, L. A chemically driven insulator–metal transition in non-stoichiometric and amorphous gallium oxide. *Nat. Mater.* **7**, 391–398 (2008).
11 Aoki, Y. Bulk mixed ion electron conduction in amorphous gallium oxide causes memristive behavior. *Nat. Commun.* **5**, 3473 (2014).
12 Kamiya, T., Nomura, K. & Hosono, H. Present status of amorphous In–Ga–Zn–O thin-film transistors. *Sci. Technol. Adv. Mater.* **11**, 044305 (2010).
13 Ueda, S., Katsuya, Y., Tanaka, M., Yoshikawa, H., Yamashita, Y., Ishimaru, S., Matsushita, Y. & Kobayashi, K. Present status of the NIMS contract beamline BL15XU at SPring-8. *AIP Conf. Proc.* **1234**, 403 (2010).
14 Ueda, S. Application of hard X-ray photoelectron spectroscopy to electronic structure measurements for various functional materials. *J. Electron. Spectrosc. Relat. Phenom.* **190**, 235–241 (2013).
15 Suresh, A., Wellenius, P., Dhawa, A. & Muth, J. Room temperature pulsed laser deposited indium gallium zinc oxide channel based transparent thin film transistors. *Appl. Phys. Lett.* **90**, 123512 (2007).
16 Nomura, K., Takagi, A., Kamiya, T., Ohta, H., Hirano, M. & Hosono, H. Amorphous oxide semiconductors for high-performance flexible thin-film transistors. *Jpn J. Appl. Phys.* **45**, 4303 (2006).
17 Heinemann, M., Berry, J., Teeter, G., Unold, T. & Ginley, D. Oxygen deficiency and Sn doping of amorphous Ga_2O_3. *Appl. Phys. Lett.* **108**, 022107 (2016).
18 Nomura, K., Kamiya, T., Yanagi, H., Ikenaga, E., Yang, K., Kobayashi, K., Hirano, M. & Hosono, H. Subgap states in transparent amorphous oxide semiconductor, In–Ga–Zn–O, observed by bulk sensitive x-ray photoelectron spectroscopy. *Appl. Phys. Lett.* **92**, 202117 (2008).
19 Ide, K., Kikuchi, Y., Nomura, K., Kimura, M., Kamiya, T. & Hosono, H. Effects of excess oxygen on operation characteristics of amorphous In-Ga-Zn-O thin-film transistors. *Appl. Phys. Lett.* **99**, 093507 (2011).
20 Orui, T., Herms, J., Hanyu, Y., Ueda, S., Watanabe, K., Sakaguchi, I., Ohashi, N., Hiramatsu, H., Kumomi, H., Hosono, H. & Kamiya, T. Charge compensation by excess oxygen in amorphous In–Ga–Zn–O films deposited by pulsed laser deposition. *J. Displ. Technol.* **11**, 518–522 (2015).
21 Kim, J., Miyokawa, N., Ide, K., Toda, Y., Hiramatsu, H., Hosono, H. & Kamiya, T. Room-temperature fabrication of light-emitting thin films based on amorphous oxide semiconductor. *AIP Adv.* **6**, 015106 (2016).

22 Hosono, H. Ionic amorphous oxide semiconductors: material design, carrier transport, and device application. *J. Non-Cryst. Solids* **352**, 851–858 (2006).
23 Klein, A. Transparent conducting oxides for photovoltaics: manipulation of fermi level, work function and energy band alignment. *Materials* **3**, 4892–4914 (2010).
24 Mohamed, M. Schottky barrier height of Au on the transparent semiconducting oxide β-Ga_2O_3. *Appl. Phys. Lett.* **101**, 132106 (2012).
25 Wei, S. & Zunger, A. Role of metal d states in II-VI semiconductors. *Phys. Rev. B* **37**, 8958 (1988).
26 Van de Walle, C. G. & Neugebauer, J. Universal alignment of hydrogen levels in semiconductors, insulators and solutions. *Nature* **423**, 626–628 (2003).
27 Robertson, J. & Clark, S. J. Limits to doping in oxides. *Phys. Rev. B* **83**, 075205 (2011).

Supplementary Information accompanies the paper on the NPG Asia Materials website (http://www.nature.com/am)